Micro Gas Turbine and Solar Parabolic Dish for distributed generation

M.J. Santos, E. Vega-Lozano, R.P. Merchán, J. García-Ferrero, A. Medina and A. Calvo Hernández
Department of Applied Physics
University of Salamanca
Plaza de la Merced, s/n – 37008 Salamanca (Spain)
Phone/Fax number:+0034 923294436, e-mail: smjesus@usal.es, eduvega@usal.es, rpmerchan@usal.es , jgferrero@usal.es, amd385@usal.es, anca@usal.es

Abstract. A thermodynamic model for a Brayton-like micro-turbine in combination with a solar parabolic dish is analyzed in order to evaluate its efficiency under any ambient condition. The thermodynamic cycle is a recuperative Brayton cycle with internal irreversibilities in the recuperator, compressor and turbine and external losses associated to the heat transfers in the solar receiver, the combustion chamber, and the environment. All the irreversibilities have been taken into account in the model with home-software elaborated using *Mathematica*®.
The model validation is done by comparison with results provided by Semprini *et al.* [1]. An analysis of hybrid and sunless performance is carried out for four different micro-turbine power outlets (30, 23, 15 and 7 kWe) and for four days of the year (corresponding to each season). The greenhouse emissions are also calculated for both off-design performance and for the four power output levels.

Key words

Solar Parabolic Dish, distributed generation, Brayton cycle, micro gas turbine, thermodynamic model.

1. Introduction

Renewable energies play a major role in today´s energy market due to the combination of fossil fuel price/reserves, increasing electricity demand, and environmental concerns [2]. Particularly significant is the concept of distributed generation, which refers to a variety of technologies that generate electricity at or near where it will be used.

Distributed generation may serve a single structure, such as a home or business, or it may be part of a micro-grid (a smaller grid that is also tied into the larger electricity delivery system). When connected to the electric utility's lower voltage distribution lines, distributed generation can help to support delivery of clean, reliable power to additional customers and reduces electricity losses along transmission and distribution lines.

Concentrated Solar Power (CSP) constitutes one suitable solution for exploiting solar resources for power generation. In this context, parabolic dish systems concentrate the solar radiation onto a point focusing receiver for small-scale power production. Given the modularity feature of such system, the scale-up is a feasible option; however, they offer a suitable solution for small-scale off-grid electrification of rural areas. These systems are usually used with Stirling engines. However, the coupling with micro-gas turbines presents a number of advantages related to the reliability of the system and the lower level of maintenance required. Besides, solar hybrid dish Brayton systems can work on solar and fuel technologies allowing stable power outputs independent of solar energy variations suitable to distributed electrical generation systems.

2. Thermodynamic Model

A scheme of the system is depicted in Fig. 1. The solar energy is collected by a parabolic dish, which concentrates it onto the receiver located at the focal point. This device transfers the solar energy to the working fluid of the gas turbine which operates on a recuperative Brayton cycle: air is compressed by a centrifugal compressor (with an isentropic efficiency ε_C, rising the temperature from T_1 to T_2), then it increases with the residual heat at the turbine recuperator (from T_2 to T_x), heated up across the solar receiver (from T_x to $T_{x'}$), heated again (if necessary) by a combustor chamber (from $T_{x'}$ to T_3), and then expanded in the turbine which drives both the compressor and the high-speed alternator (reaching a temperature T_4). The low overall pressure ratio favours that the hot gases at turbine exhaust can be used to preheat the compressor delivery air prior to entering the receiver, hence increasing the global efficiency of the system [2].
The objective of the combined system is to produce a stable power output, not relying only on solar conditions, so that it will be assumed that the turbine inlet temperature, T_3, is kept approximately constant.

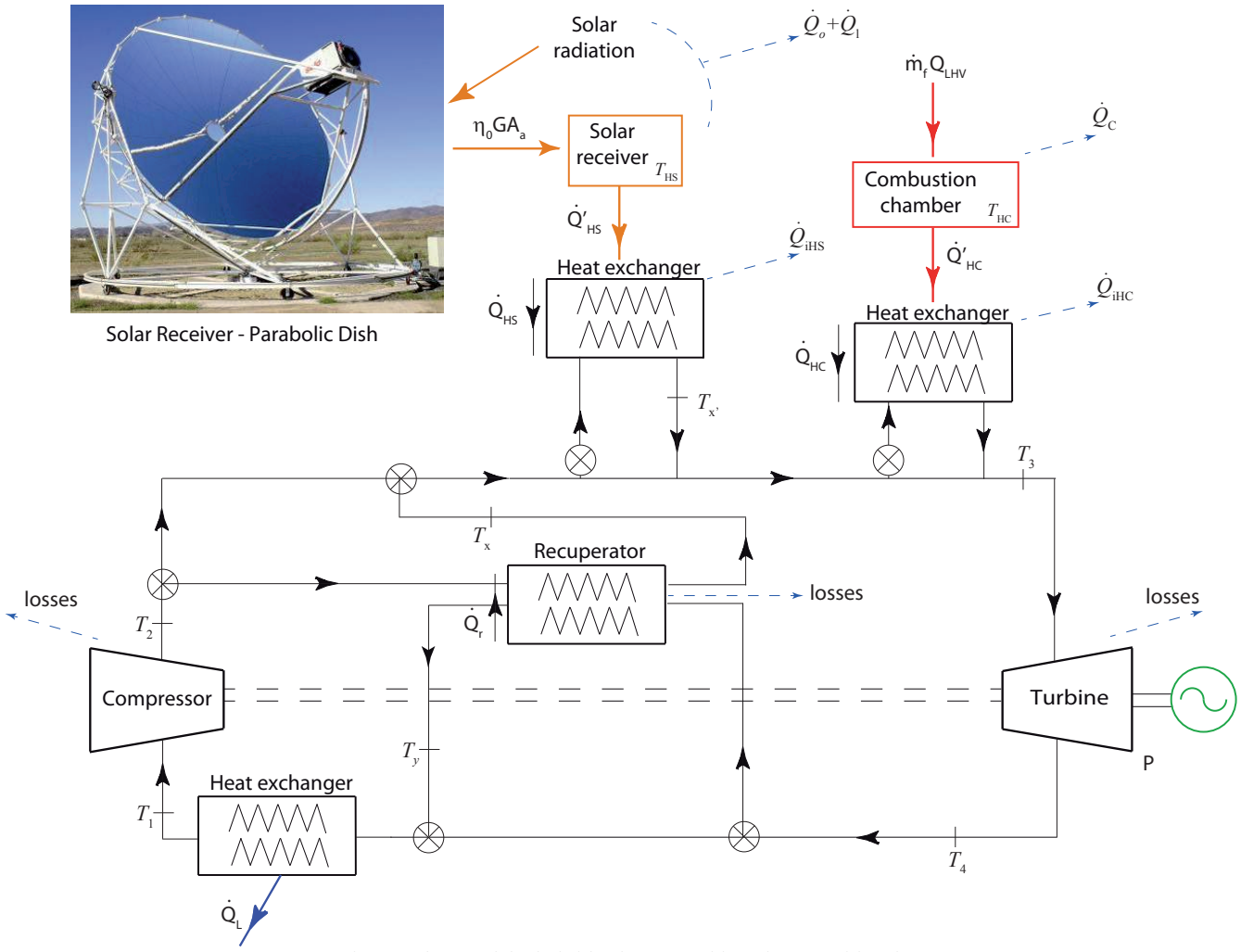

Fig. 1. Scheme of the hybrid solar gas-turbine plant considered.

A. Model

In Fig. 1 the main thermodynamic characteristics of the model are sketched: the heat transfers ($\dot{Q}'_{HS}$ heat rate transferred from the solar collector to the associated heat exchanger, $\dot{Q}_{HS}$ heat rate input from the solar subsystem to the working fluid, $\dot{Q}'_{HC}$ heat rate transferred from the combustion chamber to the associated heat exchanger, $\dot{Q}_{HC}$ heat rate input from the combustion chamber subsystem to the working fluid, $\dot{Q}_L$ heat-transfer rate between the working fluid and the ambient), temperatures of each step (as explained above), and key losses sources for each component ($\dot{Q}_o$ optical losses at the solar subsystem, $\dot{Q}_l$ losses associated to the heat transfers in the parabolic dish, $\dot{Q}_{iHS}$ heat losses at the exchanger associated with the solar receiver, $\dot{Q}_C$ heat losses at the combustion chamber, $\dot{Q}_{iHC}$ heat losses at the heat exchanger associated to the combustion chamber).

The gas turbine will be modelled as a single step recuperative closed Brayton cycle with internal irreversibilities in the compressor, turbine, recuperator, combustion chamber, and pressure drops. The overall device includes additionally the external losses and some technical details about the solar collector. A thermodynamic model implemented in *Mathematica*®, recently proposed by our group for a central tower gas turbine with a central receiver [3,4], has been adapted for the micro gas turbine coupled with a parabolic dish.

The overall thermal efficiency, η, is defined as the fraction between the net mechanical power output, P, and the global heat input rate,

$$\eta = \frac{P}{GA_a + \dot{m}_f Q_{LHV}} \tag{1}$$

where G is the direct solar irradiance, depending on the seasonal conditions, and the sun position during the day, so it is a function of time, and A_a is the aperture area of the parabolic dish (cross sectional area of the aperture plane). In addition, $\dot{m}_f$ is the fuel mass consumption rate and Q_{LHV} its corresponding lower heating value. The model allows to express also overall plant efficiency, η, as a combination of the efficiency of the plant subsystems (solar η_s, combustion η_c, and gas turbine η_h), the effectivenesses of the heat exchangers connecting subsystems (ε_{HS} for solar subsystem and ε_{HC} for combustion subsystem) and the solar share fraction (f). Thereby the overall efficiency of the whole system, η, is given by:

$$\eta = \eta_h \eta_s \eta_c \left[\frac{\varepsilon_{HS}\, \varepsilon_{HC}}{\eta_c\, f\, \varepsilon_{HC} + \eta_s\, (1-f)\, \varepsilon_{HS}} \right] \tag{2}$$

The details of the model are specified in [4].

Table I. – Parameters that are taken from Semprini *et al.*[1] both for the validation of the theoretical model and the realization of the study for four different micro-turbine power outlets.

Subsystems			*Study cases*			
			P=30 kWe ①	P=23 kWe ②	P=15 kWe ③	P=7 kWe ④
Compressor	Compressor	ε_c	0.77	0.76	0.76	0.76
Solar part	Collector	A_a (m^2)	211.8	169.4	109.6	52.80
		D_r (m)	0.3879	0.3480	0.2810	0.1941
		η_0	0.9083	0.9087	0.9092	0.9086
	Exchanger	ε_{HS}	0.7951	0.7937	0.7926	0.7923
Combustion part	Combustion chamber	η_c	0.97	0.97	0.97	0.97
	Exchanger	ε_{HC}	0.97	0.97	0.97	0.97
Turbine part	Turbine	ε_t	0.76	0.76	0.75	0.74
Regenerator part	Regenerator	ε_r	0.85	0.85	0.85	0.85
Cooling	Exchanger	ε_L	1	1	1	1
Pressure drops	Process 2→3	ρ_h	0.98	0.98	0.98	0.98
	Process 4→1	ρ_c	1	1	1	1

B. *Implementation and validation*

The validation of a thermodynamic model for a parabolic dish working with a micro gas turbine is not easy since the reported experimental results are quite scarce. Using results from Semprini *et al.* [1] our model has been validated, for solar-only not hybrid operation. Table I shows the values taken for the simulations, where ε_C is the isentropic efficiency of the compressor, D_r is the diameter of the aperture area of the receiver, η_o is the concentrator optical efficiency, ε_t is the isentropic efficiency of the turbine, ε_r is the recuperator efectiveness, ε_L is the cold side heat exchanger effectiveness, and ρ_H and ρ_L are the irreversibilities due to pressure drops in the heat input and in the heat release, respectively.

The operating conditions are determined by *direct normal irradiance*, G, and *ambient temperature*, T_L. Pressurized air will be taken as working fluid undergoing the thermal cycle. In the same way as Semprini *et al.* [1], four different micro turbine power outlets (30, 23, 15 and 7 kWe) have been considered. The numerical values used for the needed parameters in each subsystem are taken from [1]. Relative deviations for the four different cases are summarized in Table II.

Table II. – Relative deviations for the four different micro turbine power outlets (30, 23, 15 and 7 kWe), for fixed solar irradiance and ambient temperature.

Power outlets	30 kWe	23 kWe	15 kWe	7 KWe
T_L (K)	298.15	298.15	298.15	298.15
G (W/m^2)	780	780	780	780
Relative deviations				
$\Delta\eta$ (%)	6.74	7.73	7.77	7.79
$\Delta\eta_h$ (%)	8.2	8.83	8.86	8.89
ΔP (%)	7.4	9.43	9.25	9.3

The overall thermal efficiency, η, deviates between 6.7% and 7.8%. These are the values that best fit the theoretical results. The thermal efficiencies of the Brayton heat engine, η_h, are approximately the same for all cases, about 8.8%. The differences in the power generated by the turbine, P, are the greatest ones, around 9.2 %. It should be noted that the case P = 30kWe is the one showing best agreement with the reference.

The differences between our model and that of Semprini are acceptable (they are below 10% in all cases) considering that it is a pure thermodynamic model, and that the study of Semprini *et al.* [1] is quite more complex.

Table III. – Data of ambient temperature, T_L, and solar irradiance, G, for the four days of the year, at midday and at midnight.

Season	*Winter*		*Spring*		*Summer*		*Autumn*	
Day	December 21th		March 21th		June 21th		September 21th	
Hour	0 h	12 h	0 h	12 h	0 h	12 h	0 h	12 h
T_L (K)	280.35	282.95	284.55	287.75	294.05	296.55	299.95	299.35
G (W/m^2)	0	418	0	741	0	760	0	586

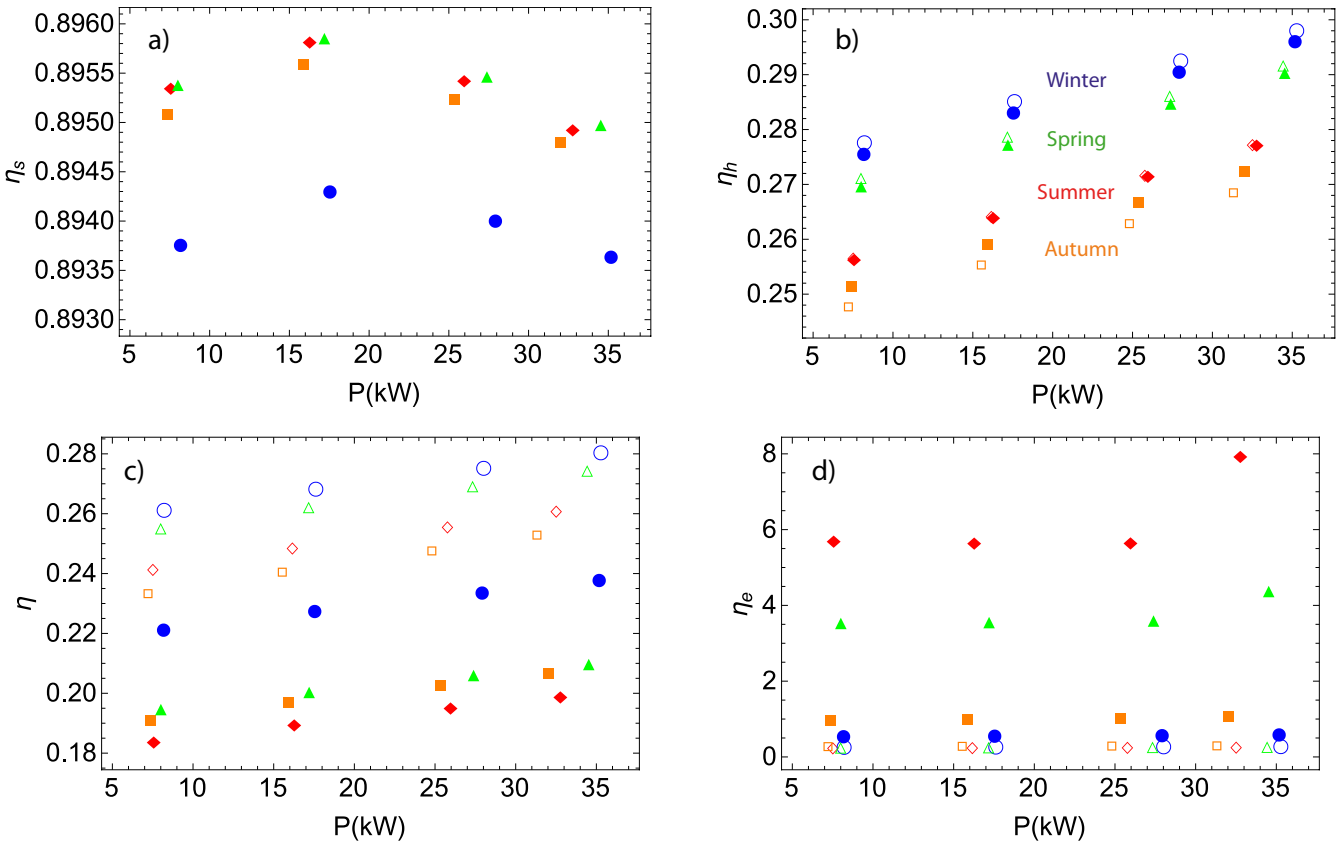

Fig. 2. Thermal efficiencies: solar collector efficiency, η_s, thermal efficiency of the Brayton heat engine, η_h, overall thermal efficiency, η, and fuel conversion rate, η_e, in function of the power, for the four days of the year. The red rhombuses represent data from the summer, the green triangles for spring, the orange squares for autumn, and the blue cycles for winter. Filled symbols refer at noon (12 hours) and empty symbols refer at midnight (0 hours).

C. Operation in real conditions

In this section a study of the solar collector behaviour, for different environmental conditions throughout the year is presented. Four representative days of the year are selected, corresponding to the four seasons: spring, summer, autumn and winter. They are, respectively, March 21th, June 20th, September 21th and December 21th, during 2013. The data of the June 20th and not the 21th are used because on this date there was a storm in Seville so that the records of ambient temperature and irradiance do not coincide with a summer peak of high intensity in the sun's rays and high temperatures.

In Table III the values of G and T_L are recorded for the four days, and for each day the two hours studied: at midday (12 hours) and at midnight (0 hours). These data are taken from the records carried out by the company Meteosevilla [5]. Below we focus on the results with special emphasis in the hybrid mode during the day and without solar contribution during the night ($G=0$). In both cases we analyse the fuel consumption and, related to it, the pollutant emissions produced by these systems when working in hybrid mode. In this way, the reduction of emissions of polluting gases can be clearly seen.

3. Results

A graphic summary of our study is presented in Fig. 2, where we plot the results obtained for the solar collector efficiency, η_s, thermal efficiency of the Brayton heat engine, η_h, overall thermal efficiency, η, and fuel conversion rate, η_e, in function of the power, for the four days of the year. In references [2] and [3] the details about these efficiencies and about the main characteristics of the model are presented. The data of the four seasons are labelled by assigning a symbol and a colour for each season: green triangles for spring, red diamonds for summer, orange squares for autumn and blue circles for winter. Filled symbols label results at noon and empty symbols at midnight.

The solar collector efficiency, η_s, versus P (Fig. 2a) presents a maximum around $P=17$ kWe, since the differences between winter and the other three seasons are minimal. They amount around 0.2%, both for the operation in hybrid mode (12 h) and without solar contribution (00 h). As expected η_s is null for midnight, as there is no heat input from the solar subsystem (therefore it has not been represented in Fig. 2a).

The thermal efficiency of the Brayton heat engine, η_h, versus P (see Fig. 2b) shows a clear behavior in all cases: it becomes higher as the power generated increases.

The overall thermal efficiency, η, (see Fig. 2c) grows as the power generated increases for each season. It should be noted that in winter, when the solar irradiance and the ambient temperature have the minimum annual values, the overall performance of the system gets the maxima values. Lower yields are obtained for operation in hybrid mode because in this case losses occur in the solar system.

The fuel conversion rate, η_e, against P (Fig. 2d) may appear to remain invariant in autumn and winter, but if a smaller scale is selected, an increase with power output is observed. The solar irradiance has a great influence on this performance because for high solar irradiance seasons (spring and summer) a large increase of η_e for the higher powers is clearly observed. During the night, when the only contribution is due to combustion, (natural gas in this case) the fuel conversion rate, η_e takes the overall performance value, $\eta_e = \eta$ (note in Fig. 2d the small scale of the night operation mode which fits the one in Fig. 2c for the overall thermal efficiency).

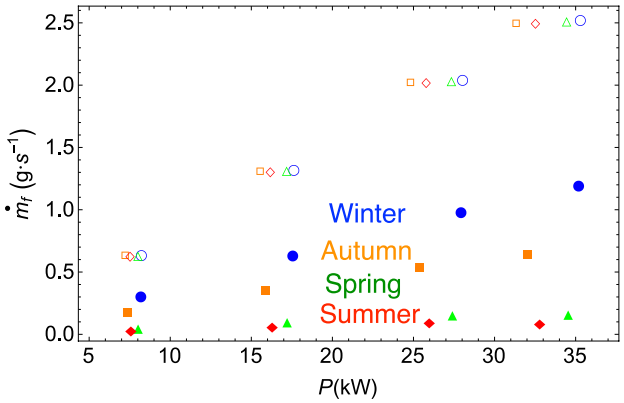

Fig. 3. Fuel consumption as a function of power, for a representative day of each season. Hybrid mode, at 12 o'clock (filled symbols) and running without sun, at 0 o'clock (empty symbols)

Natural gas has been considered as fuel, since it has the lowest emissions of pollutant gases per unit of energy produced. Fig. 3 shows fuel consumption as a function of power, for a representative day of each season. Hybrid mode, at 12 o'clock (filled symbols) and running without sun, at 0 o'clock (empty symbols). It shows how the fuel consumption increases as the output power does for the hybrid operation mode, being this increase more pronounced as we move from summer to winter, as expected according with irradiance conditions. On the other hand, during the night the behaviour is almost independent of the season of the year as it should be in the pure combustion mode at each considered power output and scales as power does.

Table IV summarizes the results for fuel consumption at 12 o'clock and at 00 o'clock, for the four different micro turbine power outlets (30, 23, 15 and 7 kWe), on December 21th, and the corresponding savings. Comparing these fuel consumption data, the hybrid mode allows fuel savings of over 50% in all cases.

Table IV. – Fuel consumption for the four different micro turbine power outlets (30, 23, 15 and 7 kWe), at 12 o'clock and at 00 o'clock, on December 21th, and the corresponding savings.

Power outlets	*30kWe*	*23kWe*	*15kWe*	*7KWe*
Fuel consumption (kg/day), December 21th				
12 h	103.0	84.6	54.5	26.2
00 h	217.7	176.2	113.8	54.7
Relative deviation				
$\Delta \dot{m}_f$ (%)	52.7	52.0	52.1	52.1

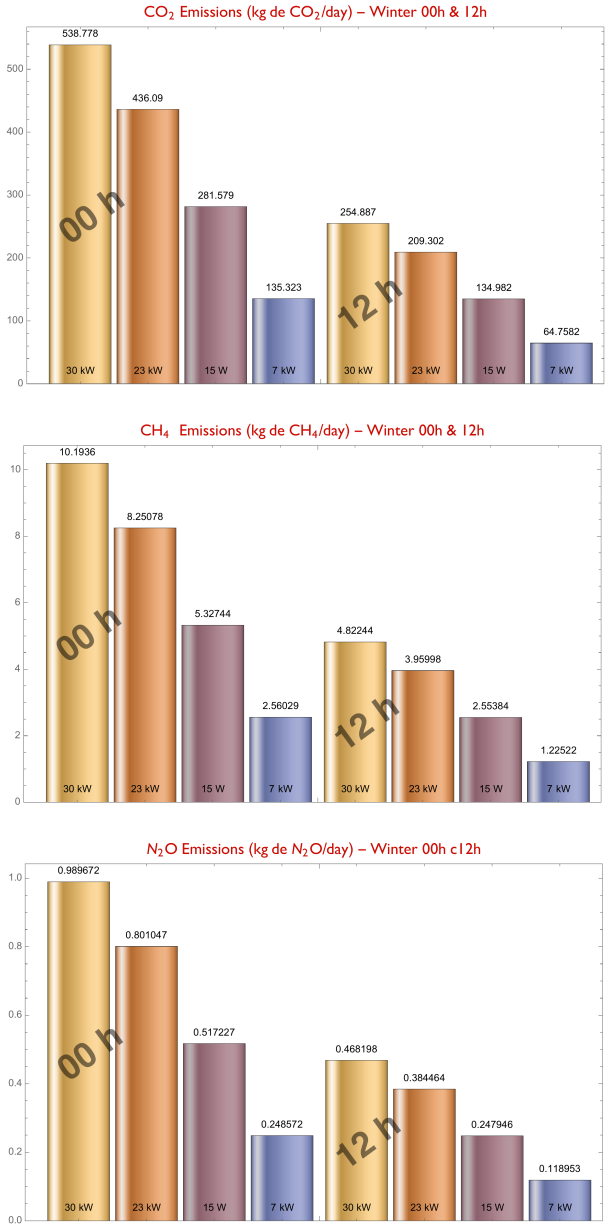

Fig. 4. Graphical representation of the emissions on December 21th at midnight (00 h) and at midday (12 h) for the four power cases.

In the combustion of natural gas there are basically three gaseous pollutants concerning greenhouse effect: carbon dioxide, methane and nitrous oxide. They are products of a chemical reaction, and therefore each will occur in a different proportion. Differences in fuel consumption between day and night are transferred directly to pollutant emissions [6]. As an example, Fig. 4 shows the results obtained for the emission of these three gases on December 21th at night (00 h) and at noon (12 h), for the four power cases. This day is elected because it presents the lowest irradiance and ambient temperature values and thus the higher fuel consumption. A comparison can be made between the two modes of operation, and so quantify the reduction of pollution. Thus, it is appreciated in Fig. 4 that for the three gases and for all output power, the hybrid mode reduces pollutant emissions by more than 50%, according to the fuel saving.

4. Conclusion

A thermodynamic model for a micro gas turbine hybridized with a solar parabolic dish has been developed. The model is divided in subsystems (see Fig. 1) and for each subsystem analytical equations for output records are obtained adapting previous works for a central tower gas turbine [3,4]. The model includes a reduced set of parameters accounting for the main irreversibilities of the power plant and it has been validated from the Semprini's model [1].

The solar dish performance is studied for four different power outputs (*P=30* kWe, *P=23* kWe, *P=15* kWe and *P=7* kWe) in a representative day of each season and for two different hours each day: at midnight (00 h) and at midday (12 h).

The differences between day and night have been studied for all cases. The seasonal representation of the efficiencies shows that the solar efficiency has a maximum around *P=17* kWe during the day (Fig. 2a), and is equal to zero at night; the thermal micro-turbine efficiency increases with the power, showing the high values at the night hours (Fig. 2b) because of the pure combustion model performance, which cancel the thermal losses coming the solar subsystem. Although global efficiency may be lower than the one associated with the turbine, both parameters behave in the same way (fig. 2c); on the opposite side, the economic performance shows (fig. 2d) higher values during the day due to the reduction of the fuel in the combustion chamber and compensated by the high irradiances specially during spring and summer times.

The aim of any solar parabolic dish technology is to decrease the consumption of fuel and of the pollutant emissions introducing hybrid technology in the energy generation process. In this line the results show a significant reduction of greenhouse emission over 50% (Fig. 4) accomplished by the corresponding reduction of fuel (Fig. 3).

In summary, the model constitutes a thermodynamic analysis of hybridized micro gas turbines in order to predict the daily and seasonal evolution of the performance of real installations in terms of a reduced set of parameters each with a clear physical meaning [4]. The reported results, which could complement previous thermo-economic models [7,8], show the suitability of hybrid dish Brayton heat engines to work on solar and fuel technologies allowing stable power outputs independent of solar energy variations as required by distributed electrical generation systems.

Acknowledgement

The authors acknowledge financial support from JCYL of Spain, Grant SA017P17.

References

[1] S. Semprini, D. Sánchez and A. De Pascale, “Performance analysis of a micro gas turbine and solar dish integrated system under different solar-only hybrid operating conditions”, Sol. Ener., 132:279-293, 2016.

[2] D. Sánchez, A. Bortkiewicz, J.M. Rodríguez, G.S. Martínez, G. Gavagnin, T. Sánchez, “A methodology to identify potential markets for small-scale solar thermal power generators”, Applied Energy, 169:287-300, 2016.

[3] D. Olivenza-León, A. Medina, and A. Calvo Hernández, “Thermodynamic modeling of a hybrid solar gas-turbine power plant”, in Energ. Conv. Manage., 93: 435-447, 2015.

[4] M.J. Santos, R.P. Merchán, A. Medina, and A. Calvo Hernández, “Seasonal thermodynamic prediction of the performance of a hybrid solar gas-turbine power plant”, in Energ. Convers. Manage., 115: 89-102, 2016.

[5] Meteosevilla. http://www.meteosevilla.com.

[6] Emission factors for greenhouse gas inventories, April 2014. https://www.epa.gov/sites/production/files/2015-07/documents/emission-factors_2014.pdf

[7] M.C. Camaretti, R. De Robbio, E. Pirone, and R. Tuccillo, “Thermo-Economic analysis of a hybrid solar micro gas turbine power plant”, in Energy Procedia., 126: 667-674, 2017.

[8] G. Gavagnin , D. Sánchez, G.S. Martínez , J.M. Rodríguez, and A. Muñoz, “Cost analysis of solar thermal power generators based on parabolic dish and micro gas turbine: manufacturing, transportation and installation”, Applied Energy, 194:108-122, 2017.